

# On the Gas-Phase Reactivity of Complexed OH<sup>+</sup> with Halogenated Alkanes

Christian Adlhart, Osamu Sekiguchi, and Einar Uggerud\*<sup>[a]</sup>

**Abstract:** OH<sup>+</sup> is an extraordinarily strong oxidant. Complexed forms (L–OH<sup>+</sup>), such as H<sub>2</sub>OOH<sup>+</sup>, H<sub>3</sub>NOH<sup>+</sup>, or iron–porphyrin–OH<sup>+</sup> are the anticipated oxidants in many chemical reactions. While these molecules are typically not stable in solution, their isolation can be achieved in the gas phase. We report a systematic survey of the influence on L on the reactivity of L–OH<sup>+</sup> towards alkanes and halogenated alkanes, showing the tremendous influence of L on the reactivity of L–OH<sup>+</sup>. With the help of with quantum chemical calculations, detailed mechanistic insights on these very general reactions are gained. The gas-phase pseudo-first-order reaction rates of H<sub>2</sub>OOH<sup>+</sup>, H<sub>3</sub>NOH<sup>+</sup>, and protonated 4-picoline-*N*-oxide towards isobutane and different halogenated alkanes C<sub>*n*</sub>H<sub>2*n*+1</sub>Cl (*n* = 1–4), HCF<sub>3</sub>, CF<sub>4</sub>, and CF<sub>2</sub>Cl<sub>2</sub> have

been determined by means of Fourier transform ion cyclotron resonance measurements. Reaction rates for H<sub>2</sub>OOH<sup>+</sup> are generally fast (7.2 × 10<sup>–10</sup>–3.0 × 10<sup>–9</sup> cm<sup>3</sup> mol<sup>–1</sup> s<sup>–1</sup>) and only in the cases HCF<sub>3</sub> and CF<sub>4</sub> no reactivity is observed. In contrast to this H<sub>3</sub>NOH<sup>+</sup> only reacts with *t*C<sub>4</sub>H<sub>9</sub>Cl (*k*<sub>obs</sub> = 9.2 × 10<sup>–10</sup>), while 4-CH<sub>3</sub>-C<sub>5</sub>H<sub>4</sub>N-OH<sup>+</sup> is completely unreactive. While H<sub>2</sub>OOH<sup>+</sup> oxidizes alkanes by an initial hydride abstraction upon formation of a carbocation, it reacts with halogenated alkanes at the chlorine atom. Two mechanistic scenarios, namely oxidation at the halogen atom or proton transfer are found. Accurate proton af-

finities for HOOH, NH<sub>2</sub>OH, a series of alkanes C<sub>*n*</sub>H<sub>2*n*+2</sub> (*n* = 1–4), and halogenated alkanes C<sub>*n*</sub>H<sub>2*n*+1</sub>Cl (*n* = 1–4), HCF<sub>3</sub>, CF<sub>4</sub>, and CF<sub>2</sub>Cl<sub>2</sub>, were calculated by using the G3 method and are in excellent agreement with experimental values, where available. The G3 enthalpies of reaction are also consistent with the observed products. The tendency for oxidation of alkanes by hydride abstraction is expressed in terms of G3 hydride affinities of the corresponding cationic products C<sub>*n*</sub>H<sub>2*n*+1</sub><sup>+</sup> (*n* = 1–4) and C<sub>*n*</sub>H<sub>2*n*</sub>Cl<sup>+</sup> (*n* = 1–4). The hypersurface for the reaction of H<sub>2</sub>OOH<sup>+</sup> with CH<sub>3</sub>Cl and C<sub>2</sub>H<sub>5</sub>Cl was calculated at the B3LYP, MP2, and G3<sub>m</sub><sup>\*</sup> level, underlining the three mechanistic scenarios in which the reaction is either induced by oxidation at the hydrogen or the halogen atom, or by proton transfer.

**Keywords:** C–H activation • gas-phase reactions • oxidation • peroxides • proton affinities

## Introduction

One strategy for the C–H activation of alkanes is mild and environmentally benign oxidation.<sup>[1]</sup> This can be achieved by reaction with hydrogen peroxide in the presence of a suitable catalyst [Eq. (1)].



This reaction also takes place in superacid solution, as demonstrated by Olah et al.<sup>[2]</sup> Results of gas-phase reactions<sup>[3]</sup> and quantum chemical calculations<sup>[4]</sup> have confirmed Olah's notion that the key step in the reaction involves a protonated hydrogen peroxide molecule, which abstracts a hydride from the alkane. In the gas phase where the excess energy<sup>[5]</sup> causes immediate dissociation of the product complex, the alkyl R<sup>+</sup> ion, is the ultimate product. The protonated hydrogen peroxide molecule, H<sub>2</sub>OOH<sup>+</sup>, can formally be regarded as a complex between water and a hydroxyl cation (incipient OH<sup>+</sup>). The free species OH<sup>+</sup> is an extremely strong oxidant, which is reflected in its high electron-recombination energy of 1257 kJ mol<sup>–1</sup> and a hydride affinity of 1932 kJ mol<sup>–1</sup> (see Table 2, below). For practical purposes, however, utiliza-

[a] Dr. C. Adlhart, Dr. O. Sekiguchi, Prof. E. Uggerud  
Department of Chemistry, University of Oslo  
P.O. Box 1033 Blindern, 0315 Oslo (Norway)  
Fax: (+47) 22-85-54-41  
E-mail: einar.uggerud@kjemi.uio.no

Supporting information for this article is available on the WWW under <http://www.chemeurj.org/> or from the author. The Supporting information contains CID spectra of selected products from the ion molecule reactions, correlation curves for calculated energies and alkyl group *a* values, G3, B3LYP/6-31G(d), MP2//B3LYP/6-31G(d), and G3<sub>m</sub><sup>\*</sup>//B3LYP/6-31G(d) energies, and cartesian coordinates of all investigated molecules.

tion of free OH<sup>+</sup> seems to be quite unrealistic. On the other hand, as demonstrated in the case of protonated hydrogen peroxide, modified forms of OH<sup>+</sup> are of interest in finding workable processes for use, for example, in industry.

Another example of incipient OH<sup>+</sup> comes from biochemistry. The enzyme families of Cytochrome P-450, methane monooxygenases, bleomycin, and porphyrin peroxidases are involved in oxidative processes in living organisms. In the oxidation reaction of such enzymes, the porphyrin prosthetic group can be regarded as a ligand that binds to OH<sup>+</sup> through its iron atom. Specific examples are the Cys<sub>357</sub>(Fe<sup>IV</sup>)porphyrin–OH<sup>+</sup> radical intermediate and the Cys<sub>357</sub>(Fe<sup>III</sup>)porphyrin–OH intermediate in the rebound mechanism<sup>[6]</sup> and in the cationic “OH<sup>+</sup>” insertion mechanism,<sup>[7]</sup> respectively. On the basis of this biological motif, a great variety of analogous organometallic systems have been studied both stoichiometrically and catalytically.<sup>[8–11]</sup>

Persistent halide-containing compounds represent an environmental problem. By substituting the halides of such molecules by a hydroxide moiety they become more soluble in water; this may prevent them from accumulating in fat tissues of higher animals. Also in this case oxidative degradation by “OH<sup>+</sup>” represents an interesting option. Normally, a C–F bond is stronger than a C–H bond, while a C–Cl bond is weaker. This puts limits on which oxidant to use in each case.

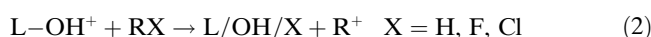
For these important reasons it would be highly interesting to learn more about the intrinsic properties of molecules which formally may be regarded as adducts with OH<sup>+</sup>. In this paper we will look at the reactivity of various small molecules that contain C–X bonds (X = H, F, Cl) with molecules of the type L–OH<sup>+</sup> (L = H<sub>2</sub>O, NH<sub>3</sub>, *p*-methyl-pyridine). It is of particular interest to study how the oxidative properties vary with the nature of the complexing molecule L. An indication comes from thermodynamic consideration, and Table 2 (see later) lists the gas-phase hydride affinities of a range of cations. Comparison will tell if hydride abstraction in a given case is thermochemically feasible or not. It is also clear from Table 2 (see later) that the hydride affinity of H<sub>2</sub>OOH<sup>+</sup> is higher than that of H<sub>3</sub>NOH<sup>+</sup>, showing that am-

monia stabilizes OH<sup>+</sup> better than water. The limitation of the thermochemical argument is of course the existence of energy barriers for reaction. This will be the topic for much of the following discussion.

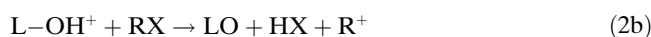
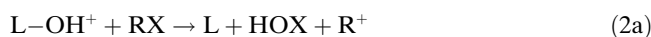
To estimate the thermochemistry of potential reaction channels a series of ab initio calculations were conducted employing the GAUSSIAN 03 suite of programs.<sup>[12]</sup>

## Results and Discussion

Table 1 summarizes reaction rates and observed products for the reaction of H<sub>2</sub>OOH<sup>+</sup>, H<sub>3</sub>NOH<sup>+</sup>, and protonated 4-picoline-*N*-oxide (L–OH<sup>+</sup>, L = H<sub>2</sub>O, NH<sub>3</sub>, or 4-CH<sub>3</sub>-C<sub>5</sub>H<sub>4</sub>N<sup>[13]</sup>) with isobutane and different halogenated alkanes. The reactions proceed either with high efficiency to complete consumption of L–OH<sup>+</sup> or the substrates remain unaffected during the observation time—from several minutes for L = H<sub>2</sub>O, due to proton transfer to background water, up to several hours for L = NH<sub>3</sub> and 4-CH<sub>3</sub>-C<sub>5</sub>H<sub>4</sub>N. In most cases we observe R<sup>+</sup> as the main product. Formation of R<sup>+</sup> corresponds to a formal hydride or chloride abstraction [Eq. (2)]



The nature of the neutral product L/OH/X remains experimentally unsettled, but the most likely outcome of the reaction in Equation (2) would be dissociation of the L–O bond to give L + HOX (X = H, F, Cl) [Eq. (2a)]. The other alternative would be proton transfer from L–OH<sup>+</sup> to RX with subsequent elimination of HX [Eq. (2b)].



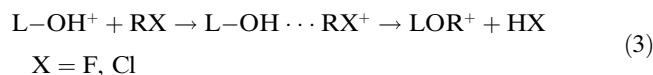
A distinction of between Equation (2a) (one-step Lewis acid) and Equation (2b) (two-step Brønsted acid) can be made based on reaction enthalpies and mechanistic considerations (vide infra).

Table 1. Reaction rates for the reaction of H<sub>2</sub>OOH<sup>+</sup> and NH<sub>3</sub>OH<sup>+</sup> with different substrates RX in the FT-ICR cell.

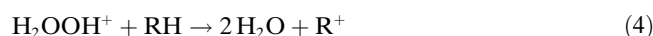
RX	L	L–OH <sup>+</sup> + RX		$\alpha^{[c]}$	X	R <sup>+</sup>	observed products and branching ratios			
		$k_{\text{obs}}^{[a]}$	$k_{\text{coll}}^{[b]}$				RO <sup>+</sup>	RH <sub>2</sub> O <sub>2</sub> <sup>+</sup>	RHCl <sup>+</sup>	RCIOH <sup>+</sup>
<i>i</i> C <sub>4</sub> H <sub>10</sub>	H <sub>2</sub> O	7.2 × 10 <sup>−10</sup>	1.5 × 10 <sup>−9</sup>	0.49	H <sup>+</sup>	1.0	–	–	–	–
HCF <sub>3</sub>	H <sub>2</sub> O	[d]								
CF <sub>4</sub>	H <sub>2</sub> O	[d]								
CF <sub>2</sub> Cl <sub>2</sub>	H <sub>2</sub> O	9.7 × 10 <sup>−10</sup>	1.4 × 10 <sup>−9</sup>	0.70	F <sup>−</sup>	–	–	1.0	–	–
CH <sub>3</sub> Cl	H <sub>2</sub> O	1.0 × 10 <sup>−9</sup>	2.4 × 10 <sup>−9</sup>	0.43	Cl <sup>−</sup>	–	–	–	–	1.0
C <sub>2</sub> H <sub>5</sub> Cl	H <sub>2</sub> O	1.6 × 10 <sup>−9</sup>	2.6 × 10 <sup>−9</sup>	0.63	Cl <sup>−</sup>	0.1	0.1	0.3	0.5 <sup>[e]</sup>	–
<i>i</i> C <sub>3</sub> H <sub>7</sub> Cl	H <sub>2</sub> O	1.3 × 10 <sup>−9</sup>	2.6 × 10 <sup>−9</sup>	0.47	Cl <sup>−</sup>	1.0	–	–	–	–
<i>t</i> C <sub>4</sub> H <sub>9</sub> Cl	H <sub>2</sub> O	3.0 × 10 <sup>−9</sup>	2.7 × 10 <sup>−9</sup>	1.11	Cl <sup>−</sup>	1.0	–	–	–	–
C <sub><i>n</i></sub> H <sub>2<i>n</i>+2</sub> ( <i>n</i> = 1–4)	NH <sub>3</sub>	[d]								
C <sub><i>n</i></sub> H <sub>2<i>n</i>+1</sub> Cl ( <i>n</i> < 4)	NH <sub>3</sub>	[d]								
<i>t</i> C <sub>4</sub> H <sub>9</sub> Cl	NH <sub>3</sub>	9.2 × 10 <sup>−10</sup>	2.7 × 10 <sup>−9</sup>	0.34	Cl <sup>−</sup>	0.1	–	0.7 <sup>[f]</sup>	0.2 <sup>[g]</sup>	–
C <sub><i>n</i></sub> H <sub>2<i>n</i>−1</sub> Cl ( <i>n</i> < 5)	<i>p</i> -NC <sub>5</sub> H <sub>4</sub> CH <sub>3</sub>	[d]								

[a] Pseudo-first-order reaction rates  $k_{\text{obs}}$  in mol<sup>−1</sup>cm<sup>3</sup>s<sup>−1</sup>, the estimated absolute error is ± 20%. [b] Theoretical collision rate according to the PTM model in cm<sup>3</sup>mol<sup>−1</sup>s<sup>−1</sup>. [c] Reaction efficiency. [d] No reaction observed. [e] The branching ratio is the sum of the RHCl<sup>+</sup> peak and a peak at *m/z* = 93, formally C<sub>4</sub>H<sub>10</sub>Cl<sup>+</sup>, to which RHCl<sup>+</sup> reacts further on. Their ratio depends on the reactant gas pressure. [f] RH<sub>2</sub>NOH<sup>+</sup>. [g] RCH<sub>3</sub>NOH<sup>+</sup>.

A second group of products, namely  $\text{RLO}^+$ , was observed for the reaction of ( $\text{L}-\text{OH}^+$ ,  $\text{L}=\text{H}_2\text{O}$  or  $\text{NH}_3$ ) with  $\text{CF}_2\text{Cl}_2$ ,  $\text{C}_2\text{H}_5\text{Cl}$ , and  $\text{C}_4\text{H}_9\text{Cl}$ . The product ions are formal  $\text{HX}$  ( $\text{X}=\text{F}$ ,  $\text{Cl}$ ) elimination products of the adduct  $\text{L}-\text{OH}\cdots\text{RX}^+$  [Eq. (3)]. Such an adduct is observed for the reaction of  $\text{H}_3\text{NOH}^+$  with  $t\text{C}_4\text{H}_9\text{Cl}$ .



In a former study, in which  $\text{H}_2\text{OOH}^+$  was treated with alkanes,<sup>[3]</sup> it was demonstrated that the reaction mechanism for the observed formation of  $\text{R}^+$  is a two-electron oxidation of the alkane substrate through  $\text{H}_2\text{OOH}^+$  under concomitant abstraction of a hydride and formation of two water molecules [Eq. (4)].



For the reaction of  $\text{L}-\text{OH}^+$  with halogenated alkanes, we have to consider additional mechanisms, namely two-electron oxidation at the halogen, as well as direct proton transfer from the acidic  $\text{L}-\text{OH}^+$  to the basic halogenated alkane. This leads to the formulation of three different reaction mechanisms, initiated by:

- A) A two-electron oxidation by hydride abstraction.
- B) A two-electron oxidation by halide abstraction.
- C) A proton transfer.

This mechanistic scenario will serve as the basis for our further discussion.

**Reaction of  $\text{H}_2\text{OOH}^+$  with  $\text{CH}_3\text{Cl}$ :** The reaction of  $\text{H}_2\text{OOH}^+$  with  $\text{CH}_3\text{Cl}$  is a special case, as the observed product  $\text{CH}_4\text{ClO}^+$  is distinct from those found for the other reactions. The product  $\text{CH}_4\text{ClO}^+$  corresponds to net transfer of  $\text{OH}^+$  from  $\text{H}_2\text{OOH}^+$  to  $\text{CH}_3\text{Cl}$  to give  $[\text{C}_2\text{H}_4\text{Cl}_2\text{O}]^+$  (**3**), Figure 1a. The structure of **3** is either the thermodynamically preferred protonated chlorohydroxymethylene  $\text{ClCH}_2\text{OH}_2^+$  (**3a**) ( $\Delta E_{\text{G3m}^*} = -314 \text{ kJ mol}^{-1}$ ) or the chloronium ion  $\text{CH}_3\text{ClOH}^+$  (**3b**) ( $\Delta E_{\text{G3m}^*} = -111 \text{ kJ mol}^{-1}$ ), Figure 2.

Fragmentation of **3** by off-resonant collision-induced dissociation (CID) leads to four cationic fragments  $\text{CH}_3^+$ ,  $\text{CH}_3\text{O}^+$ ,  $\text{CH}_4\text{O}^+$ , and  $\text{CH}_2\text{Cl}^+$  at approximately equal intensity (see Supporting Information) and therefore the assignment of **3** remains ambiguous. A third structure, the hypochloride should also be taken into account, since the potential isomerization via **TS3b/3c** requires only  $151 \text{ kJ mol}^{-1}$ , Figure 2. Independent generation of **3a** by chemical ionization of chloromethanol failed due to the instability<sup>[14]</sup> of the latter, with a lifetime of approximately 1 min.<sup>[15]</sup> Interestingly, Schriver-Mazzuoli et al. have observed  $\text{CH}_3\text{ClO}^+$ —the corresponding base of **3b**—for the reaction of an O atom with  $\text{CH}_3\text{Cl}$  in argon matrix.<sup>[16]</sup>

Formation of **3a** involves an initial 2-electron oxidation by hydride abstraction (A), whereas formation of **3b** in-

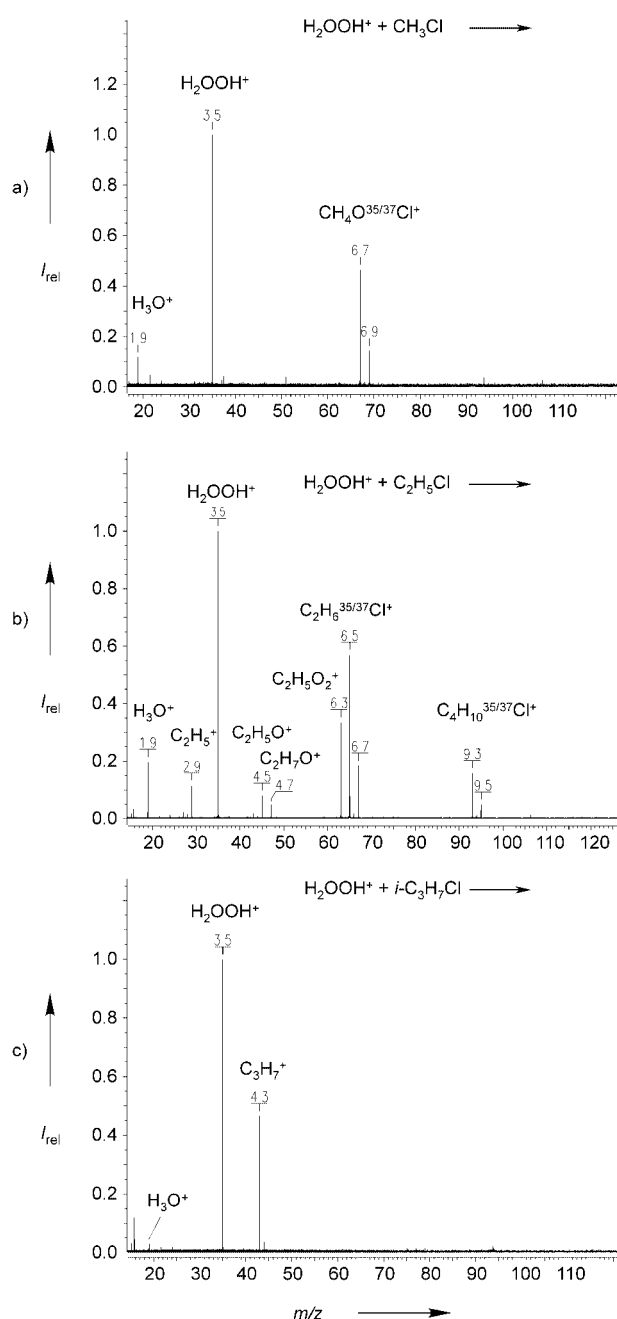


Figure 1. Reaction of  $\text{H}_2\text{OOH}^+$  with a)  $\text{CH}_3\text{Cl}$ ,  $p_{\text{obs}} = 4.6 \times 10^{-9}$  mbar, 10 s; b)  $\text{C}_2\text{H}_5\text{Cl}$ ,  $p_{\text{obs}} = 3.8 \times 10^{-9}$  mbar, 15 s; c)  $i\text{-C}_3\text{H}_7\text{Cl}$ ,  $p_{\text{obs}} = 7.8 \times 10^{-9}$  mbar, 4 s; in the FT-ICR cell. The signal for  $\text{H}_3\text{O}^+$  at  $m/z = 19$  arises from fast proton transfer to background water.

volves an initial chloride abstraction (B) (Figure 2). Direct proton transfer (C; not shown in Figure 2) can be excluded by comparing the known and calculated (G3) proton affinities of  $\text{CH}_3\text{Cl}$  and  $\text{HOOH}$ , Table 2. A proton transfer product  $\text{CH}_3\text{ClH}^+$  is only observed if  $\text{H}_2\text{OOH}^+$  is trapped in the FT-ICR cell without prior cooling by pulsed-in argon.

Although we cannot differentiate experimentally whether **3** is formed according to mechanism A or B, it is likely that the activation energy for hydride abstraction (A) from

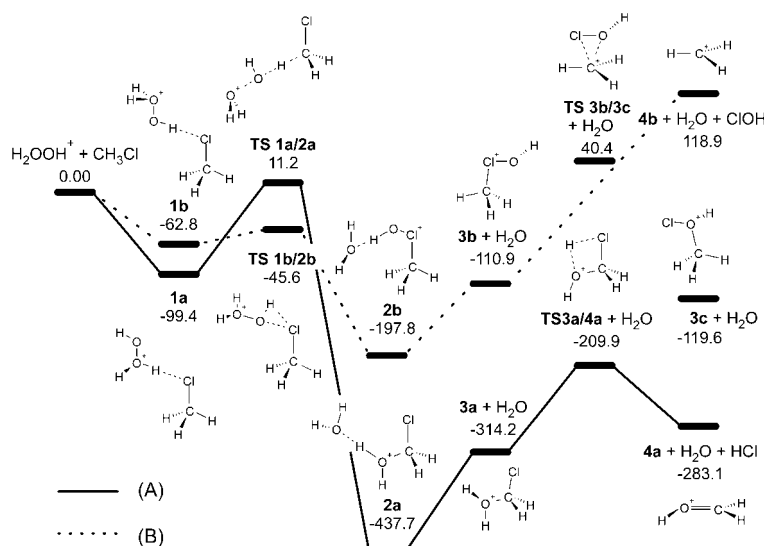


Figure 2.  $G_{3,m}^*$  energies in  $\text{kJ mol}^{-1}$  for the reaction of  $\text{H}_2\text{OOH}^+$  with  $\text{CH}_3\text{Cl}$ . A) initial hydride abstraction. B) initial oxidation at the chloride.

Table 2. Calculated  $G_3$  proton affinities ( $\text{PA}_{G_3}$ ), experimental proton affinities<sup>[19b]</sup> ( $\text{PA}_{\text{exptl}}$ ), and calculated  $G_3$  hydride affinities ( $\text{HA}_{G_3}$ ).

	$\text{PA}_{G_3}$ [ $\text{kJ mol}^{-1}$ ]	$\text{PA}_{\text{exptl}}$ [ $\text{kJ mol}^{-1}$ ]		$\text{HA}_{G_3}$ [ $\text{kJ mol}^{-1}$ ]
$\text{H}_2\text{O}$	690.2	691.0	$\text{OH}^+$	1931.8
$\text{H}_2\text{O}_2$	667.7	674.5	$\text{H}_2\text{OOH}^+[\text{a}]$	1388.3
$\text{HONH}_2$	817.3	–	$\text{HONH}_3^+[\text{b}]$	1132.1
$\text{HCF}_3$	569.0	619.5	$\text{CF}_3^+$	1278.0
$\text{CF}_4$	524.7	529.3	$\text{CF}_4$	–
$\text{CF}_2\text{Cl}_2$	654.5	–	$\text{CF}_2\text{Cl}_2$	–
$\text{CH}_3\text{Cl}$	648.1	647.3	$\text{CH}_2\text{Cl}^+$	1207.9
$\text{C}_2\text{H}_5\text{Cl}$	675.8	693.4	$\text{C}_2\text{H}_4\text{Cl}^+(\alpha)$	1121.5
$i\text{C}_3\text{H}_7\text{Cl}$	705.2	–	$i\text{C}_3\text{H}_6\text{Cl}^+(\alpha)$	1060.3
$t\text{C}_4\text{H}_9\text{Cl}$	742.9	–	$t\text{C}_4\text{H}_8\text{Cl}^+(\beta)$	1074.1
$\text{CH}_4$	539.7	543.5	$\text{CH}_3^+$	1341.6
$\text{C}_2\text{H}_6$	574.0	596.3	$\text{C}_2\text{H}_5^+$	1163.8
$\text{C}_3\text{H}_8$	618.6	625.7	$i\text{C}_3\text{H}_7^+$	1087.9
$i\text{C}_4\text{H}_{10}$	686.2	677.8	$t\text{C}_4\text{H}_9^+$	1022.5

[a]  $\text{H}_2\text{OOH}^+ + \text{H}^- \rightarrow 2\text{H}_2\text{O}$ . [b]  $\text{HONH}_3^+ + \text{H}^- \rightarrow \text{H}_2\text{O} + \text{NH}_3$ .

$\text{CH}_3\text{Cl}$  should not be higher than from  $\text{CH}_4$ . As a matter of fact, the observed rate for  $\text{CH}_3\text{Cl}$  is three orders of magnitude higher than for  $\text{CH}_4$ .<sup>[3]</sup> The rate difference cannot be explained by the higher collision rate alone (calculated according to Su's and Chesnavich's PTM model<sup>[27]</sup>), since this is only a factor of 2.2 higher, Table 1.

The computed energy diagram (Figure 2) also supports mechanism B, since the associated activation barrier is  $57 \text{ kJ mol}^{-1}$  lower than for mechanism A, although it is likely that route A is also possible.<sup>[17]</sup>

Unlike the higher alkyl chlorides,  $\text{CH}_3\text{Cl}$  does not react to give the alkyl cation. Formation of  $\text{CH}_3^+$  would involve the endothermic release of  $\text{ClOH}$  from **3b**, for which the  $G_{3,m}^*$  data shows the products to be  $119 \text{ kJ mol}^{-1}$  above the reactants (Figure 2). If **3a** were formed instead of **3b**, we could expect subsequent dissociation of **3a** into protonated form-

aldehyde **4a** plus  $\text{HCl}$ , because the calculated activation barrier for proton transfer followed by  $\text{HCl}$  elimination of  $104 \text{ kJ mol}^{-1}$ , transition state **TS 3a/4a**, is significantly lower than the  $314 \text{ kJ mol}^{-1}$  of internal energy available to **3a**. Experimentally, however, protonated formaldehyde is not observed; this result leads to the foundation of our skepticism towards mechanism A.

**Reaction of  $\text{H}_2\text{OOH}^+$  with  $i\text{C}_3\text{H}_7\text{Cl}$  and  $t\text{C}_4\text{H}_9\text{Cl}$ :**  $\text{H}_2\text{OOH}^+$  reacts with higher chloroalkanes in a distinct reaction according to Equation (2) to give  $\text{R}^+$ , Figure 1c. This reaction is analogous to the reaction of  $\text{H}_2\text{OOH}^+$  with alkanes, al-

though the experimentally observed rates for the chlorinated alkanes are faster. An evident difference between propane and isobutane and their chlorinated homologues is their proton affinity. While the proton affinities of propane and isobutane are smaller than or similar to that of  $\text{H}_2\text{O}_2$ , the proton affinities of  $i\text{C}_3\text{H}_7\text{Cl}$  and  $t\text{C}_4\text{H}_9\text{Cl}$  are significantly higher. Therefore, direct proton transfer (mechanism C) becomes a feasible alternative to the oxidation reaction channels A and B. Although we cannot distinguish between mechanisms A–C experimentally, we are tempted to consider C as the most likely reaction mechanism due to the kinetic preference for a simple proton transfer.

Indeed, for the reaction of  $\text{H}_2\text{OOH}^+$  with  $\text{C}_2\text{H}_5\text{Cl}$  (vide infra) both, the proton-transfer product  $\text{C}_2\text{H}_5\text{ClH}^+$  as well as  $\text{R}^+$  are observed, presumably because the proton-transfer reaction is less exothermic and elimination of  $\text{HCl}$  from  $\text{C}_2\text{H}_5\text{Cl}^+$  is less favorable than from  $i\text{C}_3\text{H}_7\text{ClH}^+$  and  $t\text{C}_4\text{H}_9\text{ClH}^+$ .

**Reaction of  $\text{H}_2\text{OOH}^+$  with  $\text{C}_2\text{H}_5\text{Cl}$ :** The reaction of  $\text{H}_2\text{OOH}^+$  with  $\text{C}_2\text{H}_5\text{Cl}$  gives rise to the formation of four products, Figure 1b. The most intense peak is observed for the proton-transfer product  $\text{C}_2\text{H}_5\text{ClH}^+$ . This process is almost thermoneutral, Table 2—a key point, since this indicates that the lifetime of the product complex  $\text{C}_2\text{H}_5\text{ClH}^+ \cdots \text{O}(\text{H})\text{OH}$  will be long, which is a requirement for the multistep reaction mechanisms that will be discussed in the following. While proton transfer and subsequent  $\text{HCl}$  elimination and thus formation of the carbocation  $\text{C}_n\text{H}_{2n+1}^+$  is exothermic for the secondary and tertiary carbocations ( $n=3$  and 4), it is endothermic for the ethyl cation ( $\Delta H_{G_3} = 60 \text{ kJ mol}^{-1}$ , Table 3). Therefore,  $\text{C}_2\text{H}_5\text{ClH}^+$  is not likely to eliminate  $\text{HCl}$  to give  $\text{C}_2\text{H}_5^+$  (see the Supporting Information). Alternatively,  $\text{C}_2\text{H}_5\text{ClH}^+$  can react with  $\text{C}_2\text{H}_5\text{Cl}$  in an  $\text{S}_{\text{N}}2$  reaction to form the observed product ion  $\text{C}_4\text{H}_{10}\text{Cl}^+$ , as

Table 3. G3 enthalpies of reaction ( $\Delta H_{G3}$ ) in  $\text{kJ mol}^{-1}$ . G3 enthalpies of complexation ( $\Delta H_{G3}$ ) for the neutral products are  $-26.6$  ( $\text{ClOH} + \text{H}_2\text{O}$ ),  $-15.5$  ( $\text{HCl} + \text{H}_2\text{O}_2$ ),  $-39.3$  ( $\text{ClOH} + \text{NH}_3$ ), and  $-26.9$   $\text{kJ mol}^{-1}$  ( $\text{HCl} + \text{H}_2\text{NOH}$ ).

R	$\text{CH}_3$	$\text{C}_2\text{H}_5$	$i\text{C}_3\text{H}_7$	$t\text{C}_4\text{H}_9$
$\text{RCl} + \text{H}_2\text{OOH}^+ \rightarrow \text{R}^+ + \text{ClOH} + \text{H}_2\text{O}$	126.7	-30.2	-90.6	-150.3
$\text{RCl} + \text{H}_2\text{OOH}^+ \rightarrow \text{R}^+ + \text{HCl} + \text{HOOH}$	217.3	60.4	-0.1	-59.8
$\text{RCl} + \text{H}_3\text{NOH}^+ \rightarrow \text{R}^+ + \text{ClOH} + \text{NH}_3$	382.9	226.1	165.6	105.9
$\text{RCl} + \text{H}_3\text{NOH}^+ \rightarrow \text{R}^+ + \text{HCl} + \text{H}_2\text{NOH}$	366.9	210.0	149.6	89.9

we confirmed by independent isolation experiments with  $\text{C}_2\text{H}_5\text{ClH}^+$ .

The thermodynamically most stable structure for the  $\text{C}_2\text{H}_5\text{O}^+$  product is protonated acetaldehyde (**10**). Two distinct mechanisms may lead to the formation of **10**, either an initial hydride abstraction (A) followed by elimination of HCl from the protonated chlorohydroxyethylene intermediate or a process initiated by proton transfer (C). Although mechanism A is energetically accessible, it seems rather unlikely based on the observation that the corresponding protonated formaldehyde was not observed when  $\text{H}_2\text{OOH}^+$  was reacted with  $\text{CH}_3\text{Cl}$  (vide supra). An alternative mechanism is outlined in Figure 3: After proton transfer (C), an intramolecular nucleophilic substitution reaction within the  $\text{C}_2\text{H}_5\text{ClH}^+ \cdots \text{O}(\text{H})\text{OH}$  complex may lead to elimination of HCl. According to our  $\text{G3}_{\text{m}^*}$  calculations this is a highly likely scenario, since the entropically favorable reaction of a front-side substitution of HCl by HOOH has a barrier ( $\Delta E_{\text{G3m}^*}^{\ddagger} = -1$   $\text{kJ mol}^{-1}$ ) that is at the energy of the reactants. The entropically slightly less favorable back-side substitution is even lower in potential energy. The observed peak at  $m/z = 63$  may be due to the HCl elimination product, the peroxy intermediate **7** with the molecular formula  $\text{C}_2\text{H}_7\text{O}_2^+$ . Finally, protonated acetaldehyde is formed after isomerization of **7** by two consecutive 1,2-hydrogen shifts and eventu-

al elimination of  $\text{H}_2\text{O}$  from the intermediate protonated ethyl acetal **9** ( $m/z = 63$ ), Figure 3, as suggested by Schalley et al.<sup>[18]</sup> for the fragmentation of protonated methyl hydroperoxide. The unfavorable 1,2-hydrogen shift between **7** and **8** is catalyzed by HCl, which may stay complexed with the peroxyethane intermediate **7** after the nucleophilic substitution part. It could indeed be that only the fraction of **7** that forms such an ion molecule pair with HCl reacts further on to protonated formic aldehyde, while the free **7** remains unchanged and therefore accounts for the peak at  $m/z = 63$ .

This hypothesis is supported by an off-resonant CID experiment of  $[\text{C}_2\text{H}_7\text{O}_2]^+$  in which  $\text{C}_2\text{H}_5^+$  is observed as the exclusive fragment (see Supporting Information). Upon activation of protonated methyl hydroperoxide in the kilo electron volt regime Schalley et al.<sup>[18]</sup> observed the  $\text{CH}_3^+$  and  $\text{HOOH}^+$  fragments, revealing the presence of an intact peroxide O–O bond.

Two alternative scenarios may lead to the fourth product,  $\text{C}_2\text{H}_5^+$ . Either loss of HCl from the  $\text{C}_2\text{H}_5\text{ClH}^+$  intermediate, or formation of  $[\text{C}_2\text{H}_6\text{ClO}]^+$  and elimination of HOCl. The latter is analogous to  $[\text{C}_2\text{H}_4\text{ClO}]^+$ , the exclusive product in the reaction with  $\text{CH}_3\text{Cl}$ . We are tempted to consider the second scenario as the operating for several reasons: First, the overall reaction,  $\text{C}_2\text{H}_5\text{Cl} + \text{H}_2\text{OOH}^+ \rightarrow \text{C}_2\text{H}_5^+ + \text{HCl} + \text{HOOH}$  is 60  $\text{kJ mol}^{-1}$  endothermic, whereas  $\text{C}_2\text{H}_5\text{Cl} + \text{H}_2\text{OOH}^+ \rightarrow \text{C}_2\text{H}_5^+ + \text{ClOH} + \text{H}_2\text{O}$  is 30  $\text{kJ mol}^{-1}$  exothermic, Table 3. Second, its exothermic mechanism: In analogy to  $\text{CH}_3\text{Cl}$ ,  $\text{H}_2\text{OOH}^+$  oxidizes the chloride to form  $\text{C}_2\text{H}_5\text{ClOH}^+ \cdots \text{OH}_2$  (**6b**) ( $\Delta E_{\text{G3m}^*} = -217$   $\text{kJ mol}^{-1}$ ). The transition state, **TS 5b/6b** is  $-53$   $\text{kJ mol}^{-1}$  lower in energy than the reactants.<sup>[17]</sup> Finally, the reaction does not stop at the  $\text{H}_2\text{O}$  elimination product **7b** ( $\Delta E_{\text{G3m}^*} = -134$   $\text{kJ mol}^{-1}$ ) as is observed for  $\text{CH}_3\text{ClOH}^+$  (**3b**), because ClOH elimination and formation of the carbocation  $\text{C}_2\text{H}_5^+$  is energetically more favorable than for **3b**, Table 3.

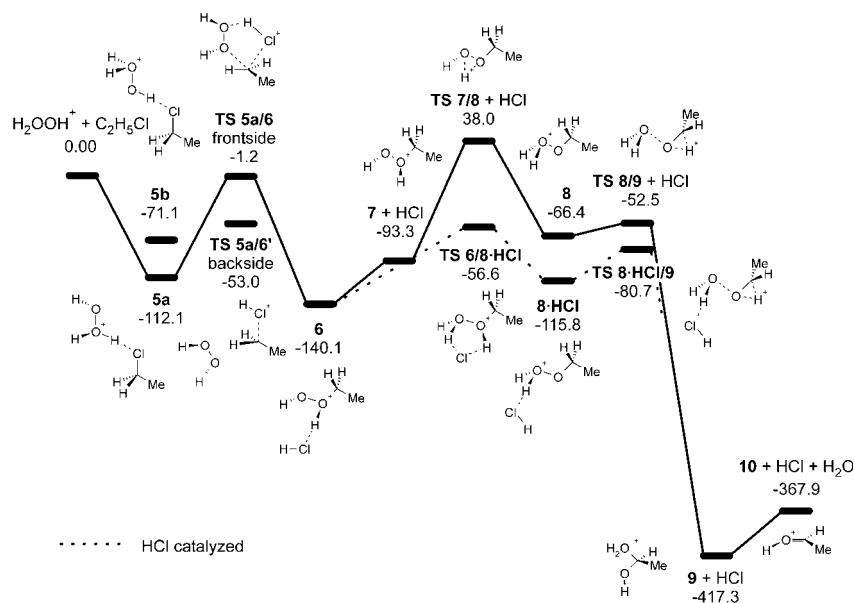


Figure 3.  $\text{G3}_{\text{m}^*}$  energies in  $\text{kJ mol}^{-1}$  are given relative to the reactants  $\text{H}_2\text{OOH}^+$  and  $\text{C}_2\text{H}_5\text{Cl}$ , including the neutral product.

**Reaction of  $\text{H}_2\text{OOH}^+$  with  $\text{CF}_2\text{Cl}_2$ :** A single product, due to loss of HF from the collision complex, was observed. We suggest that the structure is  $\text{FCl}_2\text{C}-\text{O}(\text{H})\text{OH}$  (**11**) in analogy to the HCl loss product **7** observed in the reaction between protonated hydrogen peroxide and ethyl chloride.

Because there is no  $\alpha$ -hydrogen atom available in **11**, we do not observe the following water loss product  $\text{RO}^+$ . It is clear that neither the chlorine nor the fluorine atom have the migratory ability of the hydrogen, which would be necessary to open up for water loss according to the mechanism of Figure 3.

It also interesting to note that it is HF, and not HCl, which is eliminated in the reaction between  $\text{H}_2\text{OOH}^+$  and  $\text{CF}_2\text{Cl}_2$ , despite the fact that the chlorine atoms have higher local proton affinities than the fluorine atoms. However, this difference is small ( $\Delta\text{PA}_{\text{G3}} = 7 \text{ kJ mol}^{-1}$ ).

**Reaction of  $\text{H}_3\text{NOH}^+$  with  $\text{C}_n\text{H}_{2n+1}\text{Cl}$  ( $n=1-4$ ):**  $\text{H}_3\text{NOH}^+$  did not react with isobutane or  $\text{C}_n\text{H}_{2n+1}\text{Cl}$  ( $n < 4$ ). Reaction of  $\text{H}_3\text{NOH}^+$  with  $t\text{C}_4\text{H}_9\text{Cl}$  leads to the formation of three products of which **12**,  $i\text{C}_4\text{H}_9\text{H}_2\text{NOH}^+$ , the formal HCl elimination product of the adduct, is the most abundant. Although we did not commit ourselves to the task of finding the exact structure of **12**, assuming a structure analogous to **7** and its isomers is tempting. In this respect, the observation of the initial ion molecule complex **13**,  $\text{C}_4\text{H}_9\text{Cl}\cdots\text{H}_3\text{NOH}^+$ , is also of great interest. The observation of **13** necessitates rigorous cooling of the  $\text{H}_3\text{NOH}^+$  by pulsed-in argon prior to reaction, whereupon **13** remains stable.

Complex **13** has three major reaction channels. It can either dissociate back to reform the reactants, as is underlined by the relatively low reaction efficiency of  $\alpha = 0.34$ , or, as discussed above, give rise to **12** by intramolecular nucleophilic substitution of HCl by  $\text{H}_2\text{NOH}$ . Alternatively, the weakened C–Cl bond in **13** breaks to form the neutral  $\text{H}_2\text{NOH}\cdots\text{HCl}$  complex and the observed  $t\text{C}_4\text{H}_9^+$  carbocation. Although  $t\text{C}_4\text{H}_9\text{Cl}$  is the most basic reactant in this study, Table 2, formation of  $t\text{C}_4\text{H}_9^+$  by direct proton transfer and elimination of HCl in analogy to the reaction with  $\text{H}_2\text{OOH}^+$  seems unlikely, because proton transfer from  $\text{H}_3\text{NOH}^+$  to  $t\text{C}_4\text{H}_9\text{Cl}$  is endothermic by  $74 \text{ kJ mol}^{-1}$ .

With respect to  $\text{H}_3\text{NOH}^+$ , a recently reported synthesis of  $\alpha$ - and  $\beta$ -alanine in selected ion flow tube (SIFT) experiments<sup>[19]</sup> also deserves attention. One possibility for formation of alanine in the reaction of  $\text{H}_3\text{NOH}^+$  and propionic acid is oxidation of propionic acid by  $\text{H}_3\text{NOH}^+$  through hydride abstraction and trapping of the nascent amine by the intermediate carbocation, in analogy to mechanism A. However, this assumption needs to be confirmed experimentally, and other reaction pathways involving the carboxylic group may account for the observed products.

**The role of hydride affinity:** The investigated reactions serve as a calibrant for the oxidative power of complex  $\text{OH}^+$ . In analogy to the Brønsted acidity the oxidative power can be measured in terms of hydride affinity. Complexation of  $\text{OH}^+$  by a two-electron donor, such as  $\text{H}_2\text{O}$  or  $\text{NH}_3$ , leads to a dramatic reduction of the hydride affinity from  $1932 \text{ kJ mol}^{-1}$  for  $\text{HO}^+$  to  $1388$  and  $1132 \text{ kJ mol}^{-1}$  for  $\text{H}_2\text{OOH}^+$  and  $\text{H}_3\text{NOH}^+$ , Table 2. The alkanes are the potential hydride donors in the investigated oxidation reactions, and the hydride affinity of their corresponding alkyl cations is given in Table 2. While oxidation with  $\text{H}_2\text{OOH}^+$  by hydride abstraction is exothermic for all substrates, the substrate range for  $\text{H}_3\text{NOH}^+$  is limited to higher alkanes only. This is consistent with the observed inertness of  $\text{CH}_4$  and  $\text{CH}_3\text{Cl}$  towards  $\text{H}_3\text{NOH}^+$ .<sup>[20]</sup> However, in contrast to fast proton transfer, hydride transfer affords substantial re-

arrangement of the electronic structure, which exhibits significant energy barriers. Therefore, the hydride acceptors  $\text{H}_2\text{OOH}^+$  and  $\text{H}_3\text{NOH}^+$  are not necessarily reactive, despite favorable thermochemical conditions.

According to Hammond's postulate,<sup>[21]</sup> the more exothermic reactions should show lower activation barriers for the elementary oxidation step. The activation barriers for  $\text{H}_3\text{NOH}^+$  are approximately  $110 \text{ kJ mol}^{-1}$  higher than those for  $\text{H}_2\text{OOH}^+$  and lie well above the energy of the free reactants, while the activation barrier for  $\text{H}_2\text{OOH}^+$  lies below the entering energy asymptote for all  $\text{C}_n\text{H}_{2n+1}\text{X}$  ( $\text{X} = \text{H}, \text{Cl}$ ) for  $n > 1$ , Table 4 (see also reference [4]). This readily explains why  $\text{H}_3\text{NOH}^+$  does not react with alkanes.

Table 4. B3LYP, MP2, and  $\text{G3}_{\text{m}}$  energies of activation ( $\Delta E^\ddagger$ ) including ZPVE corrections for the hydride abstraction reaction for B3LYP/6-31G(d)-optimized transition structures in  $\text{kJ mol}^{-1}$ . The reactants are taken as reference at zero energy.

	B3LYP		MP2		$\text{G3}_{\text{m}}$	
	X=H	X=Cl	X=H	X=Cl	X=H	X=Cl
$\text{H}_2\text{OOH}^+ + \text{CH}_3\text{X}$	-15.6	-13.4	23.7	27.5	13.4	11.2
$\text{H}_2\text{OOH}^+ + \text{C}_2\text{H}_5\text{X}$	-25.7	-33.0	-5.0	4.8	-13.6	-12.3
$\text{H}_3\text{NOH}^+ + \text{CH}_3\text{X}$	124.4	104.7	179.1	156.1	145.7	126.0
$\text{H}_3\text{NOH}^+ + \text{C}_2\text{H}_5\text{X}$	68.5	74.2	121.0	114.3	98.4	101.6

In contrast to alkanes, halogenated alkanes can also be oxidized at the halogen. This process appears to be favorable at least for fluoride and chloride ions. In the case of chlorine, this is governed by the equilibria given in Equations (5) and (6) in which, again,  $\text{HOOH}$  is the stronger oxidant and the oxidation of HCl is exothermic, while it is endothermic for  $\text{H}_2\text{NOH}$ .



Table 3 gives the G3 reaction enthalpies for the chloride oxidation (HOCl elimination) and proton transfer (HCl elimination) for the reaction of  $\text{L-OH}^+$  ( $\text{L} = \text{H}_2\text{O}, \text{NH}_3$ ) with  $\text{C}_n\text{H}_{2n+1}\text{Cl}$ . The above-mentioned equilibria are reflected in the favored chloride oxidation for  $\text{H}_2\text{OOH}^+$  versus a favored proton transfer for  $\text{H}_3\text{NOH}^+$ . While only the reactions of  $\text{H}_2\text{OOH}^+$  with  $i\text{C}_3\text{H}_7\text{Cl}$  and  $t\text{C}_4\text{H}_9\text{Cl}$  are clearly exothermic, consistent with the experimentally exclusively observed  $i\text{C}_3\text{H}_7^+$  and  $t\text{C}_4\text{H}_9^+$ , the reactions of  $\text{H}_2\text{OOH}^+$  with  $\text{C}_2\text{H}_5\text{Cl}$  and  $\text{H}_3\text{NOH}^+$  with  $t\text{C}_4\text{H}_9\text{Cl}$  are borderline cases, and, accordingly, only a minor fraction of the  $\text{C}_2\text{H}_5^+$  and  $t\text{C}_4\text{H}_9^+$  products are observed. A part of the anticipated endothermicity of  $90 \text{ kJ mol}^{-1}$  for the elimination of HCl and  $\text{H}_2\text{NOH}$  is neutralized by formation of a complex of the latter.

The computed hydride affinities linearly correlate with alkyl group  $a$  constants,<sup>[22]</sup> the gas-phase analogues of Taft's  $\sigma^*$  constants<sup>[23]</sup> (see the Supporting Information). The  $a$  constants were derived from alkyl cation affinities of small two-electron donors as  $\text{H}_2\text{O}$  or  $\text{Cl}^-$ . They are basically a measure for the capability of an alkyl group to stabilize a positive charge and their positive correlation with the hydride affinity is reasonable. It is also interesting to obtain a positive linear correlation with the energies of activation for the potential oxidation of hydrocarbons with  $\text{H}_3\text{NOH}^+$  by hydride abstraction. The reduced slope indicates that the charge transfer to the nascent alkyl cation is not complete in the TS.

## Conclusion

Three main conclusions can be drawn from the reactivity of complexed hydroxyl cation,  $\text{L-OH}^+$  ( $\text{L}=\text{H}_2\text{O}$ ,  $\text{NH}_3$ ), towards alkanes and halogenated alkanes. Firstly, the ligand  $\text{L}$  has strong influence on the reactivity of  $\text{L-OH}^+$ . This is reflected in the experimentally observed low reactivity of  $\text{H}_3\text{NOH}^+$  relative to the analogue  $\text{H}_2\text{OOH}^+$ . Secondly,  $\text{H}_2\text{OOH}^+$  reacts with alkanes by hydride abstraction, while it reacts with chlorinated alkanes by chloride abstraction. This suggests that  $\text{H}_2\text{OOH}^+$  may be an effective low-cost detoxicant for problematic persistent halogenated hydrocarbons. Thirdly, the tendency for hydride abstraction from alkanes and alkyl halides, as well as halide abstraction by  $\text{L-OH}^+$  increases with increasing methyl substitution in the substrate molecule.

## Experimental Section

$\text{HOOH}_2^+$  and  $\text{NH}_3\text{OH}^+$  ions were produced from a urea hydrogen peroxide addition compound (Aldrich) and hydroxylamine hydrochloride, respectively, in an external ion source using chemical ionization with methane. The ions formed in the source were transferred to the cell of an FT-ICR mass spectrometer, a Bruker 4.7 T Bio Apex (Billerica, Massachusetts, USA). Substrates, chloromethane 99.5%, chloroethane 99.7%, 2-chloropropane 99+%, 2-chloro-2-methylpropane (Aldrich), tetrafluoromethane 2.8, trifluoromethane 2.8 (Linde), and  $\text{CF}_2\text{Cl}_2$  (Freon R12, Alfax), were leaked into the cell at constant pressure ( $p=2.0\times 10^{-9}$ – $1.5\times 10^{-7}$  mbar) through a leak valve. Ion isolation and all subsequent isolation steps were performed by using a computer-controlled ion-ejection protocol, which combines single-frequency ion-ejection pulses with frequency sweeps. Briefly, all ions except the chosen reactant ion were ejected from the cell by this procedure. The remaining population of  $\text{HOOH}_2^+$  or  $\text{NH}_3\text{OH}^+$  ions was cooled to ambient temperature upon introduction of a short pulse of argon (peak-pressure,  $p=1\times 10^{-6}$  mbar). The reactant ions were then again isolated by single, optimized frequency shots that removed ions formed during the cooling period of 3 s. After this process, the ions were treated with the respective substrate for a randomly varied time before a mass spectrum was recorded. In this way products formed in ion-molecule reactions could be observed, the reaction could be followed as a function of time, and rate coefficients were obtained by fitting pseudo-first-order kinetic models to the reactant decay (absolute intensity). The substrate pressure was read out through a cold cathode ion gauge that was calibrated against the reaction of  $\text{NH}_3^+$  (generated externally by EI) plus  $\text{NH}_3$ ,  $k_r=2.2\times 10^{-9}$   $\text{cm}^3\text{mol}^{-1}\text{s}^{-1}$ <sup>[24]</sup> and

corrected by relative sensitivity factors of  $R(\text{NH}_3)=1.12$ ,  $R(i\text{C}_4\text{H}_{10})=3.23$ ,  $R(\text{CCl}_2\text{F}_2)=3.16$ ,  $R(\text{CH}_3\text{Cl})=2.22$ ,  $R(\text{C}_2\text{H}_5\text{Cl})=2.92$ ,  $R(i\text{C}_3\text{H}_7\text{Cl})=3.90$ ,  $R(t\text{C}_4\text{H}_9\text{Cl})=4.80$ .<sup>[25]</sup> While branching ratios are very precise, the estimated error of the absolute gas phase rates is  $\pm 20\%$ . The accuracy of our reaction rates was confirmed by the reaction of  $\text{CH}_5^+$  with  $t\text{C}_4\text{H}_9\text{Cl}$ , which is known to proceed at collision rate.<sup>[26]</sup> The observed rate was  $k_r=2.7\pm 0.2\times 10^{-9}$   $\text{cm}^3\text{mol}^{-1}\text{s}^{-1}$ , in agreement with the theoretical collision rate ( $2.66\times 10^{-9}$   $\text{cm}^3\text{mol}^{-1}\text{s}^{-1}$ , calculated according to Su's and Chesnavich's PTM model<sup>[27]</sup>), and the FT-ICR rate obtained by Su and Bowers  $k_r=3.28\pm 0.49\times 10^{-9}$   $\text{cm}^3\text{mol}^{-1}\text{s}^{-1}$ .<sup>[26]</sup>

Collision-induced dissociation mass spectra of selected products were recorded after off-resonant ion activation (offset=1000 Hz, duration=120  $\mu\text{s}$ ) with a simultaneous short pulse of argon ( $p=1\times 10^{-6}$  mbar) and a pumping delay of 2 s.

In order to estimate the energetics of potential reaction channels a series of ab initio calculations were conducted employing the GAUSSIAN 03<sup>[12]</sup> suite of programs. Initially, Becke three-parameter Lee-Yang-Parr (B3LYP) DFT calculations were done with the 6-31G(d) basis sets. All stationary points were subject to complete geometry optimization, including a check for the correct number of negative Hessian eigenvalues. For a restricted number of molecules, the B3LYP/6-31G(d) method was evaluated against higher basis sets (6-31++G(d,p)) and levels of theory (MP2, G2,<sup>[28]</sup> and G3<sup>[29]</sup>); critical complexation energies deviated by 30  $\text{kJmol}^{-1}$  in the worst case. To obtain more accurate estimates for the energies, G3 theory calculations were used. As expected, the proton affinities were in excellent agreement ( $<2$   $\text{kJmol}^{-1}$ ) with those obtained by Ma et al.,<sup>[30]</sup> who applied a modified G3 methodology. The G3 method is a composite technique that involves several geometry optimizations at the HF and MP2(full) level. Since many of the optimized critical point structures deviated substantially on those levels, we modified the G3 scheme such that structures were optimized on the B3LYP/6-31(G) level and ZPVE corrections were obtained from scaled (scaling factor=0.9434<sup>[31]</sup>) MP2/6-31(G) frequencies. For a further description see reference [32]. We use  $\text{G3}_{\text{m}^*}$  as notation for the modified G3 scheme. The G3 and  $\text{G3}_{\text{m}^*}$  energies of reaction for the reaction given in Equation (7) are  $\Delta E_{\text{G3}}=-91.0$   $\text{kJmol}^{-1}$  and  $\Delta E_{\text{G3}_{\text{m}^*}}=-89.1$   $\text{kJmol}^{-1}$ , respectively, in excellent agreement with the experimental estimate of  $\Delta H_r^0=-87.9$   $\text{kJmol}^{-1}$ .<sup>[33a]</sup>



The molecules were treated in their singlet electronic state throughout, as the corresponding triplet state energies of the involved closed shell molecules are even higher than the barriers on the singlet surface.<sup>[34]</sup>

## Acknowledgements

The authors wish to thank the NFR (Norwegian Research Council) for financial support through a postdoctoral fellowship for C.A. We are also grateful for a generous grant of computing time from NOTUR (the Norwegian High Performance Computing Consortium).

- [1] P. T. Anastas, T. C. Williamson, *Green Chemistry—Frontiers in Benign Chemical Syntheses and Processes*, Oxford University Press, Oxford, **1998**.
- [2] a) G. A. Olah, D. G. Parker, N. Yoneda, *J. Am. Chem. Soc.* **1977**, *99*, 483–488; b) G. A. Olah, D. G. Parker, N. Yoneda, *Angew. Chem.* **1978**, *90*, 962–984; c) G. A. Olah, T. Keumi, J. C. Lecoq, A. P. Fung, J. A. Olah, *J. Org. Chem.* **1991**, *56*, 6148–6151.
- [3] Å. M. Øiestad, A. C. Petersen, V. Bakken, J. Vedde, E. Uggerud, *Angew. Chem.* **2001**, *113*, 1345–1349; *Angew. Chem. Int. Ed.* **2001**, *40*, 1305–1309.
- [4] R. D. Bach, M.-D. Su, *J. Am. Chem. Soc.* **1994**, *116*, 10103–10109.
- [5] In exothermic gas-phase reactions, the excess reaction enthalpy cannot be released into the surrounding medium as in solution.

- “Hot” intermediates release their internal energy by three different mechanisms, such as dissociation and transformation of the internal energy into translational energy, radiative processes, and at higher pressure by collisions.
- [6] J. T. Groves, G. A. McClusky, *J. Am. Chem. Soc.* **1976**, *98*, 859–861.
- [7] M. Newcomb, P. H. Toy, *Acc. Chem. Res.* **2000**, *33*, 449–455.
- [8] a) F. A. Cotton, G. Wilkinson, *Advanced Inorganic Chemistry*, Wiley, New York, **1988**; b) J. Everse, K. E. Everse, M. B. Grisham, *Peroxidases in Biology and Chemistry*, CRC, Boca Raton, **1991**.
- [9] a) G. R. Ortiz de Montellano, *Cytochrome P-450. Structure, Mechanism and Biochemistry*, Plenum, New York, **1986**; b) L. Que, Jr., R. Y. N. Ho, *Chem. Rev.* **1996**, *96*, 2607–2624; c) M. Costas, K. Chen, L. Que, Jr., *Coord. Chem. Rev.* **2000**, *200–202*, 517–544; d) M. Costas, M. P. Mehn, M. P. Jensen, L. Que, Jr., *Chem. Rev.* **2004**, *104*, 939–986; e) S. Shaik, M. Filatov, D. Schröder, H. Schwarz, *Chem. Eur. J.* **1998**, *4*, 193–199; f) A. Marques, M. di Matteo, M.-F. Ruasse, *Can. J. Chem.* **1998**, *76*, 770–775; g) B. Meunier, A. Sorokin, *Acc. Chem. Res.* **1997**, *30*, 470–476; h) T. G. Traylor, F. Xu, *J. Am. Chem. Soc.* **1990**, *112*, 178–186.
- [10] a) M. Fontecave, S. Menage, C. Duboc-Toia, *Coord. Chem. Rev.* **1988**, *178–180*, 1555–1572; b) C. E. MacBeth, R. Gupta, K. R. Mitchell-Koch, V. G. Young, Jr., G. H. Lushington, W. H. Thompson, M. P. Hendrich, A. S. Borovik, *J. Am. Chem. Soc.* **2004**, *126*, 2556–2567.
- [11] a) K. Srinivasan, P. Michaud, J. K. Kochi, *J. Am. Chem. Soc.* **1986**, *108*, 2309–2320; b) D. Feichtinger, D. A. Plattner, *Angew. Chem.* **1997**, *109*, 1796–1798; *Angew. Chem. Int. Ed. Engl.* **1997**, *36*, 1718–1719; c) D. A. Plattner, *Top. Curr. Chem.* **2003**, *225*, 153–203.
- [12] Gaussian 03, Revision B.04, M. J. Frisch, G. W. Trucks, H. B. Schlegel, G. E. Scuseria, M. A. Robb, J. R. Cheeseman, J. A. Montgomery, Jr., T. Vreven, K. N. Kudin, J. C. Burant, J. M. Millam, S. S. Iyengar, J. Tomasi, V. Barone, B. Mennucci, M. Cossi, G. Scalmani, N. Rega, G. A. Petersson, H. Nakatsuji, M. Hada, M. Ehara, K. Toyota, R. Fukuda, J. Hasegawa, M. Ishida, T. Nakajima, Y. Honda, O. Kitao, H. Nakai, M. Klene, X. Li, J. E. Knox, H. P. Hratchian, J. B. Cross, C. Adamo, J. Jaramillo, R. Gomperts, R. E. Stratmann, O. Yazyev, A. J. Austin, R. Cammi, C. Pomelli, J. W. Ochterski, P. Y. Ayala, K. Morokuma, G. A. Voth, P. Salvador, J. J. Dannenberg, V. G. Zakrzewski, S. Dapprich, A. D. Daniels, M. C. Strain, O. Farkas, D. K. Malick, A. D. Rabuck, K. Raghavachari, J. B. Foresman, J. V. Ortiz, Q. Cui, A. G. Baboul, S. Clifford, J. Cioslowski, B. B. Stefanov, G. Liu, A. Liashenko, P. Piskorz, I. Komaromi, R. L. Martin, D. J. Fox, T. Keith, M. A. Al-Laham, C. Y. Peng, A. Nanayakkara, M. Challacombe, P. M. W. Gill, B. Johnson, W. Chen, M. W. Wong, C. Gonzalez, J. A. Pople, Gaussian, Inc., Pittsburgh PA, **2003**.
- [13] The nitrogen atom in H<sub>2</sub>NOH is 109 kJ mol<sup>-1</sup> more basic than the oxygen atom.<sup>[34a]</sup> Picoline-*N*-oxide is most likely protonated on the oxygen atom although protonation on the nitrogen atom or pyridine ring cannot be excluded.
- [14] G. Olah, A. Pavlath, *Acta Chim. Acad. Sci. Hung.* **1953**, *3*, 203–207.
- [15] G. S. Tyndall, T. J. Wallington, M. D. Hurley, W. F. Schneider, *J. Phys. Chem.* **1993**, *97*, 1576–1582.
- [16] L. Schriver-Mazzuoli, A. Schriver, Y. Hannachi, *J. Phys. Chem. A* **1998**, *102*, 10221–10229.
- [17] The B3LYP and MP2 structures for **TS 1b/2b** show a significant difference. While the oxygen and chlorine atoms are almost collinear for the MP2 structure, the B3LYP structure gives an early transition state with some remaining H–Cl interaction (2.22 Å) and the oxygen and chlorine atoms are 32° offline. Their difference in energy is, however, small: –45.6 kJ mol<sup>-1</sup> G<sub>3,m</sub>//B3LYP/6-31G(d) and –42.0 kJ mol<sup>-1</sup> G<sub>3,m</sub>//MP2/6-31G(d) for **TS 1b/2b**; –52.9 kJ mol<sup>-1</sup> G<sub>3,m</sub>//B3LYP/6-31G(d) and –49.9 kJ mol<sup>-1</sup> G<sub>3,m</sub>//MP2/6-31G(d) for **TS 5b/6b**.
- [18] C. A. Schalley, M. Dieterle, D. Schröder, H. Schwarz, E. Uggerud, *Int. J. Mass Spectrom. Ion Processes* **1997**, *163*, 101–119.
- [19] V. Blagojevic, S. Petrie, D. K. Bohme, *Mon. Not. R. Astron. Soc.* **2003**, *339*, L7–L11.
- [20] OH<sup>+</sup> would react with alkanes by one-electron rather than by two-electron oxidation due to its high electron affinity of 13 eV.
- [21] G. S. Hammond, *J. Am. Chem. Soc.* **1955**, *77*, 334–338.
- [22] E. Uggerud, *Eur. J. Mass Spectrom.* **2000**, *6*, 131–134.
- [23] a) R. W. Taft Jr., *J. Am. Chem. Soc.* **1953**, *75*, 4231–4238; b) R. W. Taft, Jr., *Steric Effects in Organic Chemistry*, Wiley, New York, **1956**.
- [24] a) Y. Ikezoe, S. Matsuoka, M. Takebe, A. Viggiano, *Gas-Phase Ion-Molecule Reaction Rate Constants Through 1986*, Maruzen, Tokyo, **1987**; b) N. G. Adams, D. Smith, J. F. Paulson, *J. Chem. Phys.* **1980**, *72*, 4951–4957.
- [25] J. E. Bartmess, R. M. Georgiadis, *Vacuum* **1983**, *33*, 149–153.
- [26] T. Su, M. T. Bowers, *J. Am. Chem. Soc.* **1973**, *95*, 7609–7610.
- [27] T. Su, W. J. Chesnavich, *J. Chem. Phys.* **1982**, *76*, 5183–5185.
- [28] L. A. Curtiss, K. Raghavachari, G. W. Trucks, J. A. Pople, *J. Chem. Phys.* **1991**, *94*, 7221–7230.
- [29] L. A. Curtiss, K. Raghavachari, P. C. Redfern, V. Rassolov, and J. A. Pople, *J. Chem. Phys.* **1998**, *109*, 7764–7776.
- [30] N. L. Ma, K.-C. Lau, S.-H. Chien, W.-K. Li, *Chem. Phys. Lett.* **1999**, *311*, 275–280.
- [31] A. P. Scott, L. Radom, *J. Phys. Chem.* **1996**, *100*, 16502–16513.
- [32] J. K. Laerdahl, E. Uggerud, *Org. Biomol. Chem.* **2003**, *1*, 2935–2942.
- [33] a) NIST Standard Reference Database Number 69 - March, 2003 Release, <http://webbook.nist.gov/chemistry/>; b) E. P. Hunter, S. G. Lias, *J. Phys. Chem. Ref. Data* **1998**, *27*, 413–656.
- [34] a) E. L. Øiested, E. Uggerud, *Int. J. Mass Spectrom. Ion Processes* **1999**, *185–187*, 231–240; b) E. L. Øiested, J. N. Harvey, E. Uggerud, *J. Phys. Chem. A* **2000**, *104*, 8382–8388.

Received: July 8, 2004

Published online: November 12, 2004